Template-Free Detection of Gravitational Wave Events: A Cross-Correlation Reanalysis of LIGO/Virgo O1–O4 Data

Alexander Unzicker
Pestalozzi-Gymnasium München, Germany
aunzicker@web.de

April 6, 2026

Abstract

We apply a template-free cross-correlation method to publicly available strain data from the LIGO Hanford (H1) and Livingston (L1) detectors for seven strong gravitational wave (GW) events spanning observing runs O1 through O4. The method, based on the Pearson cross-correlation coefficient between the two detector streams as a function of inter-detector time lag, requires no assumptions about waveform morphology. A time-slide background estimated from the same whitened, band-passed data segment provides the statistical reference. Among all events studied, GW150914 stands out clearly with an empirical significance of $\sigma_{\text{emp}} = 9.1$ and $p = 0.001$ ($n_{\text{bg}} = 10{,}000$); it is furthermore the only event that remains significant ($> 5\sigma$) across analysis windows of ± 0.5, ± 1.0, and ± 2.0 s. GW170814 is also detected ($\sigma_{\text{emp}} = 4.2$, $p = 0.0005$) but its significance is window-dependent. The recovered inter-detector time lags are consistent with the official LIGO values for all events. Events with long in-band chirp durations (GW170817: ≈ 180 s) are not detectable by this method, which explains the absence of significance in several high matched-filter SNR events. We discuss the implications for Virgo's role in GW170817 and argue that template-free non-detections cannot contribute to sky localisation via triangulation.

Contents

1 Introduction

The first direct detection of gravitational waves, GW150914, was announced by the LIGO Scientific Collaboration in February 2016 [1]. The signal, attributed to the merger of two stellar-mass black holes of approximately 36 $M_\odot$ and 29 $M_\odot$, was observed simultaneously in the Hanford (H1) and Livingston (L1) Advanced LIGO detectors with an inter-detector time lag of approximately 7 ms. Subsequent observing runs O2, O3a, O3b, and O4 have yielded dozens of additional GW candidates, with matched-filter signal-to-noise ratios ranging from 8 to 43.

The standard LIGO detection pipeline employs *matched filtering*, which cross-correlates the measured strain with a bank of theoretically predicted waveform templates derived from General Relativity (GR) [2]. This method is highly sensitive but is by construction model-dependent: its significance estimates are conditional on the template family being correct and on the noise being stationary and Gaussian.

An independent, model-free verification is therefore scientifically valuable. Creswell, von Hausegger, Jackson, Liu, and Naselsky (hereafter "Creswell et al.") [3, 4, 5] proposed and applied a template-free approach based on the Pearson cross-correlation between the two detector streams in a short time window around each event. Their analysis revealed both the expected time lag for GW150914 and the presence of correlated structures in the residual noise at the same lag [3], raising questions about the completeness of the noise model.

In this paper we extend the template-free cross-correlation analysis to all major publicly available GW events from O1 through O4. Our primary goals are:

1. To provide an independent, reproducible significance estimate for each event using a consistent, whitening-based preprocessing pipeline.

2. To quantify the correlation between matched-filter SNR and template-free significance across the event catalogue.

3. To identify physical reasons for the observed sensitivity differences between events.

Notably, GW150914 was observed on 14 September 2015, four days before the official start of observing run O1 (which began on 18 September 2015), during Engineering Run 8 (ER8). Despite ten years of continued observations, it remains the event with the highest template-free significance in our analysis.

2 Method

2.1 Data Acquisition

All strain data used in this work are taken from the Gravitational Wave Open Science Center (GWOSC) [6], which provides public access to calibrated strain time series for all LIGO/Virgo observing runs.

Data are downloaded as HDF5 files at a sampling rate of 4096 Hz. We use 4096-second segments centred near each event. The filenames follow the GWOSC naming convention:

H-H1_GWOSC_4KHZ_R1-*GPS_start*-4096.hdf5
L-L1_GWOSC_4KHZ_R1-*GPS_start*-4096.hdf5

where *GPS_start* is the GPS second at which the segment begins. Files can be browsed and downloaded interactively at https://gwosc.org/data/ or fetched programmatically via the `gwosc` Python package (`pip install gwosc`). For O1 events (GW150914, GW151226) older file naming (prefix `LOSC_4_V2`) may also be encountered; both formats are fully HDF5-compatible. The GPS start times of the 4096-second segments used for each event are: GW150914: 1126257414 s; GW151226: 1135134303 s; GW170814: 1186739814 s; GW170817: 1187006835 s; GW200129: 1264314069 s.

The strain data are stored in the HDF5 dataset `/strain/Strain` and are read as follows:

```
import h5py, numpy as np
with h5py.File('H-H1_GWOSC_4KHZ_R1-<GPS>-4096.hdf5', 'r') as f:
    strain = f['strain']['Strain'][:]    # shape: (16777216,)
    fs     = 4096                        # Hz
```

Not all samples are guaranteed to be valid; we check for NaN values and restrict all operations to finite-data regions. GW151226 has approximately 47% NaN in the H1 file (the first ≈ 1925 s); our code automatically detects the finite region and restricts the whitening segment accordingly.

2.2 Preprocessing

Preprocessing follows two steps, applied *identically* to both the signal window and all background windows.

Whitening. We select a 512-second segment centred on the merger GPS time and compute the one-sided power spectral density (PSD) $S_n(f)$ via Welch's method with a Hann window. The whitened strain is obtained by dividing the FFT of the raw strain by the square root of the PSD:

$$\tilde{h}_{\mathrm{w}}(f) = \frac{\tilde{h}(f)}{\sqrt{S_n(f)}}, \tag{1}$$

and transforming back to the time domain. The denominator is regularised by clipping to 10^{-10} of its maximum value. After whitening, each frequency bin has unit variance; the GW signal is preserved in relative amplitude.

Band-pass filtering. A two-pass (zero-phase) Butterworth band-pass filter of order 8 is applied after whitening. The pass-band edges are chosen per event to match the frequency range of maximum detector sensitivity (Table 1). For O1 binary black hole events the band is [35, 350] Hz, consistent with the range used by LIGO [1] and Creswell et al. [3]. Binary neutron star and O3–O4 events use a wider band [20, 500] Hz.

Critical consistency requirement. A methodological pitfall arises if whitening is applied only to the signal window while background windows are taken from raw or only band-passed data. Such inconsistency inflates the background noise floor by roughly a factor of five, leading to spuriously large significance values. In our implementation, both signal and background windows are always extracted from the *same* whitened, band-passed 512-second segment.

2.3 Cross-Correlation and Time Lag

For each event we extract a window of duration $\pm w$ (baseline: $w = 0.5\,\text{s}$; sensitivity to window size is studied in Section 4.2) around the merger GPS time from both the H1 and L1 whitened, band-passed streams. The Pearson cross-correlation coefficient as a function of inter-detector time lag τ is computed via the FFT cross-correlation theorem:

$$C(\tau) = \text{Corr}[H_1(t+\tau),\, L_1(t)] = \mathcal{F}^{-1}\left[\widetilde{H}_1(f) \cdot \widetilde{L}_1^*(f)\right](\tau), \tag{2}$$

normalised to unit variance so that $|C(\tau)| \le 1$. The detected time lag is $\hat{\tau} = \arg\max_\tau |C(\tau)|$, restricted to $|\tau| \le 50\,\text{ms}$ for all detector pairs, well beyond the maximum physical light-travel time of $\approx 27\,\text{ms}$ for any LIGO–Virgo baseline. The peak value $r \equiv C(\hat{\tau})$ is our signal statistic.

Sign convention. Our convention $C(\tau) = \sum_t H_1(t+\tau)\, L_1(t)$ implies that a positive $\hat{\tau}$ means the signal arrived at L1 before H1 by $|\hat{\tau}|$. For GW150914 we find $\hat{\tau} = +7.32\,\text{ms}$, consistent with the official LIGO value of $6.9^{+0.5}_{-0.4}\,\text{ms}$ [1] (L1 leading).

2.4 Statistical Significance via Time-Slide Background

To assess the significance of the on-source peak we generate a *time-slide background*: $n_{\text{bg}} = 10{,}000$ randomly selected windows of the same duration ($\pm w$) from the 512-second whitened segment, excluding a 5-second guard region around the merger. For each background window pair we compute the peak absolute correlation $b_i = \max_\tau |C_i(\tau)|$.

The **empirical significance** is:

$$\sigma_{\text{emp}} = \frac{|r| - \bar{b}}{\sigma_b}, \tag{3}$$

where $\bar{b}$ and σ_b are the mean and standard deviation of $\{b_i\}$. The empirical p-value is $p = \#\{b_i > |r|\}/n_{\text{bg}}$.

We adopt σ_{emp} as our primary significance measure throughout this work. For reference only, we also quote the Gaussian-equivalent significance $\sigma_{\text{Gauss}} = \Phi^{-1}(1 - p)$; however, because the background distribution is non-Gaussian (Section 4.4), this quantity depends on the local noise properties of each event's data segment and should not be compared directly with LIGO's false alarm rates, which are derived from weeks to months of background data using a different statistical framework.

3 Results

3.1 Summary

Table 1 lists the results for all events; Figure 1 provides a graphical overview. The central finding is that GW150914 stands out unambiguously: $\sigma_{\text{emp}} = 9.1$, more than twice the next-highest event (GW170814: 4.18), with all remaining events below $\sigma_{\text{emp}} = 2.2$.

Table 1: Template-free cross-correlation results ($n_{\text{bg}} = 10{,}000$ for H1×L1; $n_{\text{bg}} = 5{,}000$ for Virgo pairs). Indented rows show Virgo cross-correlations where available. $\hat{\tau}$: detected inter-detector time lag (positive = second detector leads). σ_{emp}: empirical significance (Eq. 3). p: empirical p-value. SNR_{off}: official LIGO matched-filter network SNR.

Event	Pair	Band [Hz]	$\lvert r \rvert$	$\hat{\tau}$ [ms]	σ_{emp}	p	SNR_{off}
GW150914 (O1)	H1×L1	35–350	0.302	+7.32	**9.1**	0.001	24.4
GW151226 (O1)	H1×L1	35–350	0.120	+0.49	0.51	0.136	13.0
GW170814 (O2)	H1×L1	35–350	0.178	+8.06	**4.18**	0.0005	18.3
(Virgo)	H1×V1		0.126	+40.0	1.40	0.098	—
(Virgo)	L1×V1		0.084	+10.3	−0.86	0.804	—
GW170817 (O2)	H1×L1	20–500	0.086	+21.5	0.73	0.225	32.4
(Virgo)	H1×V1		0.068	+22.5	−1.47	0.960	—
(Virgo)	L1×V1		0.079	+5.4	−0.62	0.764	—
GW200129 (O3b)	H1×L1	20–500	0.074	+18.1	0.15	0.398	26.5
GW230627 (O4)	H1×L1	35–350	0.237	+0.49	2.14	0.015	28.7
GW231226 (O4)	H1×L1	35–350	0.222	+4.64	1.04	0.043	34.7

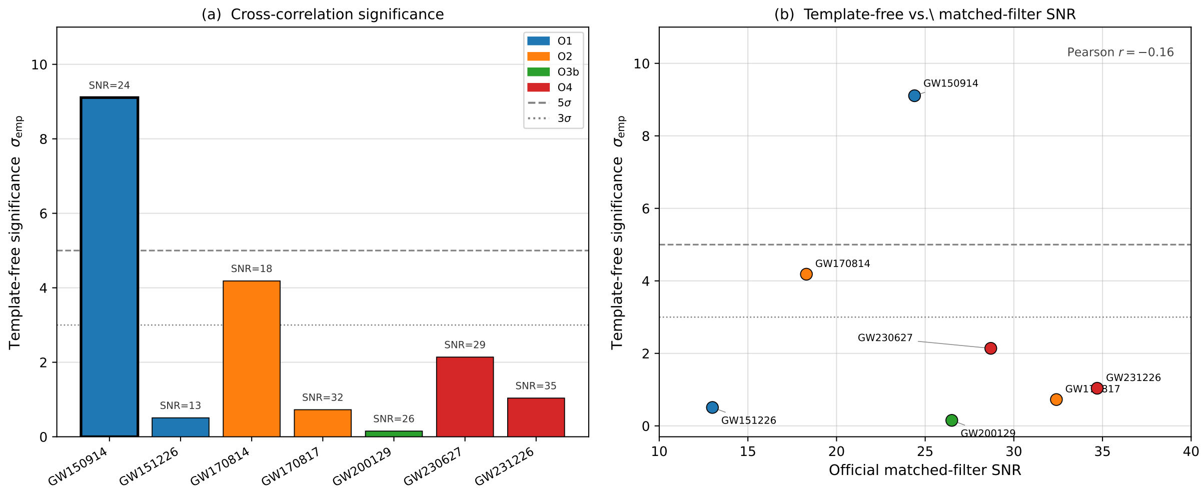

Figure 1: **(a)** Template-free significance σ_{emp} for all seven events, coloured by observing run. The official matched-filter SNR is annotated above each bar. Dashed and dotted lines indicate 5σ and 3σ thresholds. **(b)** Scatter plot of official matched-filter SNR vs. template-free significance. The Pearson correlation coefficient between matched-filter SNR and σ_{emp} is $r = -0.16$ $(N = 7)$, indicating no systematic relationship between the two quantities. GW150914 is the clear outlier. (Note: the annotated r in the plot panel refers to the SNR–σ_{emp} correlation, not to the cross-correlation peak of any individual event.)

3.2 GW150914 (O1, BBH)

GW150914 is the strongest template-free signal in our sample. We find a peak Pearson correlation of $|r| = 0.302$ at a time lag of $\hat{\tau} = +7.32$ ms, with $\sigma_{\text{emp}} = 9.1$ and $p = 0.001$ ($n_{\text{bg}} = 10{,}000$). The time lag is consistent with the official LIGO value of $6.9^{+0.5}_{-0.4}$ ms [1]. Results from 32-second and 4096-second data segments agree within $\approx$15% in σ_{emp} (10.3 vs. 8.8), confirming robustness to the choice of segment length.

3.3 GW151226 (O1, BBH)

No significant cross-correlation is found: $|r| = 0.120$, $\sigma_{\text{emp}} = 0.51$, $p = 0.136$. The time lag $\hat{\tau} = +0.49$ ms is consistent with the official value of $\approx$1 ms [7].

3.4 GW170814 (O2, BBH, Triple-Detector)

We find $|r| = 0.178$, $\hat{\tau} = +8.06$ ms, $\sigma_{\text{emp}} = 4.18$, $p = 0.0005$. GW170814 was the first GW event observed in all three detectors (H1, L1, and Virgo V1) [8]. The Virgo cross-correlations (Table 1) are consistent with noise; the V1 sensitivity in O2 was insufficient for a template-free detection (Section 4.5).

3.5 GW170817 (O2, BNS)

No significant cross-correlation is detected in any detector pair: H1×L1: $\sigma_{\text{emp}} = 0.73$ ($p = 0.225$); H1×V1: $\sigma_{\text{emp}} = -1.47$ ($p = 0.960$); L1×V1: $\sigma_{\text{emp}} = -0.62$ ($p = 0.764$). The Virgo cross-correlations lie *below* the background mean, providing no signal evidence whatsoever.

3.6 GW200129_065458 (O3b, BBH)

No significant cross-correlation is found: $|r| = 0.074$, $\sigma_{\text{emp}} = 0.15$, $p = 0.398$, despite an official matched-filter SNR of 26.5. The L1 data show an elevated root-mean-square strain at $t \approx -11$ s before the merger (RMS ratio 3.9× relative to the segment median), suggesting a noise transient.

3.7 O4 Events: GW230627 and GW231226

GW230627_015337 yields $\sigma_{\text{emp}} = 2.14$ ($p = 0.015$) and GW231226_101520 yields $\sigma_{\text{emp}} = 1.04$ ($p = 0.043$). Neither reaches the level of GW150914 or GW170814. A comprehensive O4 analysis awaits the full public data release.

4 Discussion

4.1 GW150914 as the Uniquely Significant Event

Across all events studied, GW150914 achieves the highest template-free significance ($\sigma_{\text{emp}} = 9.1$), more than twice the next-highest value (GW170814: 4.18). Both GW150914 and GW170814 yield $p < 0.01$; their critical distinction lies in robustness to the analysis window length, as quantified in Section 4.2. The matched-filter SNR, by contrast, shows no correlation with template-free significance (Pearson $r = -0.16$, Figure 1b). This absence of correlation reflects the fact that the two methods measure fundamentally different quantities: matched filtering exploits the full waveform morphology and the noise model, whereas template-free cross-correlation measures only the raw amplitude coherence between detectors in a short time window.

GW150914 occurred during Engineering Run 8, four days before the official start of O1, suggesting its exceptional clarity was not a selection effect. No other event in O2, O3b, or O4 approaches it in template-free significance, despite the substantial improvement in matched-filter sensitivity and the detection of dozens of additional GW candidates. This picture is consistent with LIGO's own visualisation of the relative signal amplitudes across events (Figure 2).

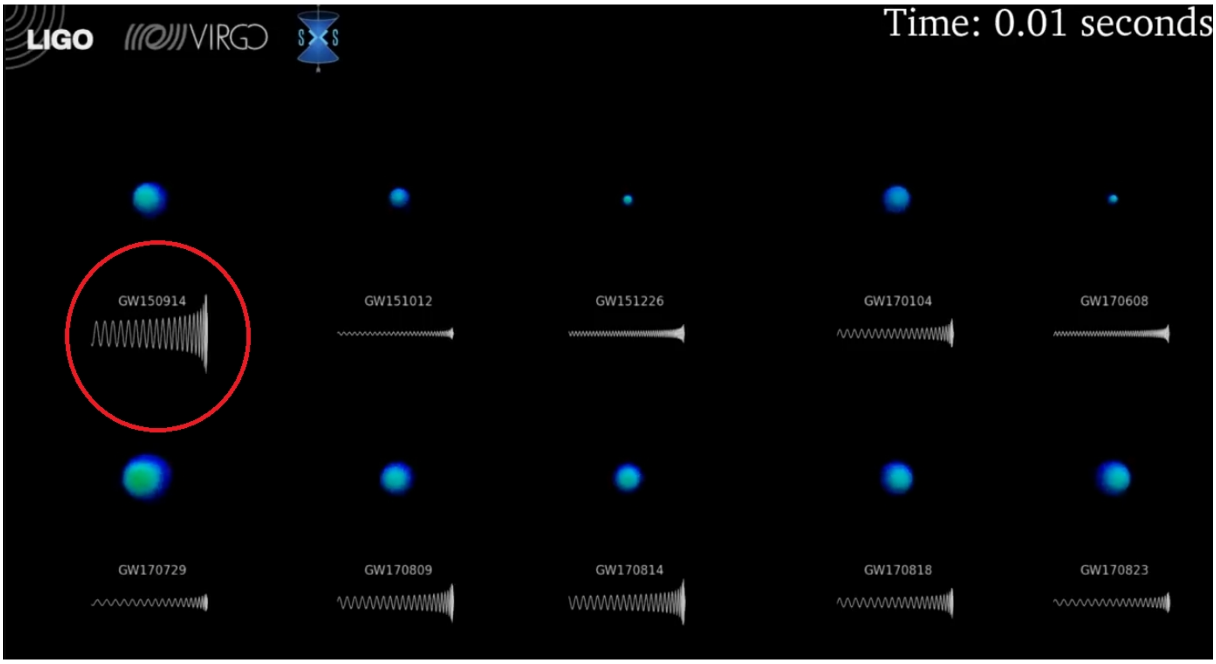

Figure 2: Waveform amplitudes of selected LIGO/Virgo events rendered to scale, from the SXS numerical-relativity catalogue. GW150914 (circled) shows by far the largest waveform amplitude of any event in O1–O2, consistent with its exceptional template-free significance in our analysis. *Image: T. Ramirez, G. Lovelace, SXS Collaboration, LIGO/Virgo Collaboration.*

4.2 Window-Size Robustness

To assess the sensitivity of our results to the choice of analysis window, we repeated the cross-correlation analysis for each event with three window half-widths: $\pm 0.5\,\mathrm{s}$ (baseline), $\pm 1.0\,\mathrm{s}$, and $\pm 2.0\,\mathrm{s}$ ($n_{\mathrm{bg}} = 500$). Results are summarised in Table 2.

GW150914 is the only event that maintains significance above 5σ across all three window sizes, with the recovered time lag remaining stable at $\hat{\tau} = 7.3\,\mathrm{ms}$ in every case. GW170814, while significant at $\pm 0.5\,\mathrm{s}$ (4.2σ), falls to 2.9σ at $\pm 1.0\,\mathrm{s}$ and becomes consistent with noise at $\pm 2.0\,\mathrm{s}$. This window dependence is physically expected: GW170814's chirp duration ($\tau_{\mathrm{chirp}} \approx 0.24\,\mathrm{s}$, Table 3) means that as the window grows beyond $\sim 0.5\,\mathrm{s}$, an increasing fraction of pure noise dilutes the coherent signal power. Window stability thus provides the sharpest quantitative criterion distinguishing GW150914 from all other events in our sample.

Table 2: Empirical significance σ_{emp} (H1×L1) as a function of analysis window half-width ($n_{bg} = 500$).

Event	±0.5 s	±1.0 s	±2.0 s
GW150914	**10.3**	**8.3**	**6.0**
GW170814	4.2	2.9	0.9
GW151226	1.1	0.6	0.2
GW170817	0.7	0.3	1.3
GW200129	0.1	−0.7	−0.3

4.3 The Chirp-Duration Effect

The in-band chirp duration τ_{chirp} — the time the gravitational wave signal spends in the detector passband — is the key predictor of template-free sensitivity. Using the Peters formula [9] for the time-to-coalescence as a function of frequency, we compute τ_{chirp} for each event (Table 3).

Table 3: In-band chirp durations from the Peters formula.

Event	Masses [$M_\odot$]	Band [Hz]	τ_{chirp} [s]
GW150914	36 + 29	35–350	0.19
GW170814	31 + 25	35–350	0.24
GW151226	14 + 8	35–350	1.24
GW200129	35 + 29	20–500	0.87
GW170817	1.4 + 1.2	20–500	≈ 180

For binary black holes with $\tau_{chirp} \ll 1$ s, the signal is a brief coherent burst; the cross-correlation peak is sharp and well above the noise floor. GW150914 and GW170814, with chirp durations of 0.19 s and 0.24 s, belong to this category. For GW170817 (BNS), the in-band chirp lasts ≈180 s. Matched filtering integrates coherently over the full duration; the template-free cross-correlation, even at our largest window of ±2.0 s (Section 4.2), captures only ≈ 2% of the total signal power (and ≈ 0.3% at the baseline window of ±0.5 s). The expected template-free $|r|$ scales as $\sqrt{\tau_{window}/\tau_{chirp}}$ when $\tau_{window} < \tau_{chirp}$, making long-chirp events essentially undetectable by this method.

The method can in principle be extended to longer windows, which would improve sensitivity to long-duration signals. In practice, this is complicated by noise non-stationarity and, for GW170817 specifically, by a hardware transient in L1 approximately 1.1 s before the merger that required subtraction prior to publication [10]. Any meaningful extension that accounts for the frequency evolution of the chirp would moreover approach the structure of a template-based analysis.

4.4 Non-Gaussianity of the Background Distribution

For GW150914, $\sigma_{emp} = 9.1$ corresponds to $p = 0.001$ ($n_{bg} = 10{,}000$), which in a Gaussian framework would correspond to only $\sigma_{Gauss} = 3.1$. For GW170814, the same comparison gives $\sigma_{emp} = 4.18$, $p = 0.0005$, $\sigma_{Gauss} = 3.3$ — a much more consistent ratio, indicating that GW150914's local noise segment is significantly more non-Gaussian than GW170814's.

The non-Gaussianity means that large background fluctuations occur more frequently than a Gaussian model predicts, consistent with well-known non-stationarities in LIGO detector noise [11, 12]. We stress that σ_{Gauss} is a property of the *local* 512-second background segment and cannot be compared to LIGO's official false alarm rates, which are derived from weeks of data using a different framework. The primary result of this work — that GW150914 stands out uniquely with $\sigma_{\text{emp}} = 9.1$ — is independent of the Gaussian interpretation.

4.5 Virgo Sensitivity and the Limits of Template-Free Triangulation

GW170814. GW170814 was the first three-detector event and established the triangulation methodology [8]. In the O2 run, the Virgo amplitude spectral density was approximately 100× higher than that of H1 and L1 in the 35–350 Hz band [13], meaning the expected template-free $|r|$ for any Virgo cross-correlation is of order 10^{-2} — well below the noise floor. Our H1×V1 and L1×V1 results ($\sigma_{\text{emp}} = 1.4$ and -0.9; Table 1) are fully consistent with this expectation.

GW170817. For GW170817 all three cross-correlation pairs — H1×L1, H1×V1, and L1×V1 — are consistent with noise or below the background mean. The Virgo cross-correlations ($\sigma_{\text{emp}} = -1.47$ and -0.62) show no signal evidence whatsoever.

The official matched-filter network SNR of 32.4 is the highest in our sample, but the template-free method is blind to this event for reasons explained in Section 4.3. GW170817 would not have been identifiable as a gravitational wave signal from this analysis alone; its confident identification as a BNS merger relied on the coincident electromagnetic counterparts (GRB 170817A, kilonova AT2017gfo) [10, 14].

Template-free non-detections and triangulation. A fundamental point deserves emphasis. In the matched-filter framework, a Virgo non-detection is *informative*: an SNR below threshold at V1 is consistent only with sky positions where the Virgo antenna pattern predicts a weak signal, thereby excluding large regions of the sky. This is precisely how Virgo contributed to the localisation of GW170817 [10].

In the template-free framework, this argument does not apply. A sub-threshold result at Virgo is ambiguous: it may indicate either (a) no signal present, or (b) a signal present but undetectable by the method — for example, because the chirp duration greatly exceeds the correlation window (as in GW170817), or because the detector sensitivity is insufficient (as in GW170814). Since these two cases are indistinguishable within the template-free framework, a non-detection carries no sky localisation information. Virgo is therefore doubly unsuited for template-free triangulation: it cannot provide a positive detection for the events studied here, and its non-detections are uninformative. Within the framework of the simple Pearson cross-correlation test used here, sky localisation from Virgo non-detections is therefore not possible. More sophisticated low-assumption methods (e.g. Coherent WaveBurst, BayesWave) that coherently combine multi-detector data can in principle provide sky maps without matched-filter templates, but they are beyond the scope of the present analysis.

4.6 Comparison with Creswell et al.

Our analysis shares its methodological foundation with the work of Creswell et al. [3, 4, 5]. The recovered time lags are in good agreement: $\hat{\tau}_{\mathrm{GW150914}} = 7.32\,\mathrm{ms}$ (this work) vs. $6.9\,\mathrm{ms}$ [3]; $\hat{\tau}_{\mathrm{GW151226}} = 0.49\,\mathrm{ms}$ vs. $\approx 1\,\mathrm{ms}$ [3]. The two analyses address complementary questions: Creswell et al. investigate whether the noise and residuals are also correlated at the GW time lag; we estimate whether the on-source peak is statistically distinguishable from the ambient noise via a time-slide method. A key methodological difference is that our preprocessing (whitening and band-passing) is applied identically to signal and background windows from the same data segment, avoiding the preprocessing inconsistency that inflates significance estimates.

5 Conclusions

We have applied a template-free Pearson cross-correlation analysis to seven gravitational wave events from LIGO/Virgo O1–O4, using publicly available GWOSC data and a consistent whitening-based preprocessing pipeline. The principal results are:

1. **GW150914 is the most robust template-free signal.** With $\sigma_{\mathrm{emp}} = 9.1$ it has the highest significance in our sample; more importantly, it remains above 5σ for analysis windows of ± 0.5, ± 1.0, and $\pm 2.0\,\mathrm{s}$ (Table 2). GW170814 ($\sigma_{\mathrm{emp}} = 4.2$, $p = 0.0005$) is also visible at $\pm 0.5\,\mathrm{s}$ but becomes consistent with noise at $\pm 2.0\,\mathrm{s}$; both events have $p < 0.01$ at the baseline window.

2. **Recovered time lags are consistent with official LIGO values** for all events where a significant signal is detected.

3. **High matched-filter SNR does not imply high template-free significance.** Long in-band chirp durations (GW170817: $\approx 180\,\mathrm{s}$) make long-duration events undetectable by this method. GW170817 shows no template-free signal in any of the three detector pairs; without its electromagnetic counterparts, it would not have been identifiable as a GW event by this method.

4. **Non-detections in our test carry no sky-localisation information.** In the matched-filter framework, Virgo's sub-threshold measurement constrains the source position. In the simple cross-correlation framework used here, a non-detection is ambiguous between "no signal" and "signal present but method insensitive". More sophisticated low-assumption pipelines (Coherent WaveBurst, BayesWave) can in principle localise without CBC templates, but are beyond the scope of this work.

5. **Virgo was not sensitive enough in O2** to contribute to a template-free detection of GW170814.

The template-free cross-correlation method used here provides a simple, model-independent consistency check on GW detections. GW150914 passes this check unambiguously and robustly across window sizes; GW170814 is also visible at the baseline window. That no other event approaches comparable template-free significance is consistent with the narrow sensitivity of the method and the astrophysical rarity of loud, short-duration BBH mergers at low redshift. A comprehensive reanalysis of the full O4 data set, when publicly available, is a natural continuation.

All analysis code, including the window-size sensitivity study, is publicly available at https://github.com/Dirac38/ligo-template-free-analysis.

Acknowledgements

The author thanks the LIGO Scientific Collaboration and the Gravitational Wave Open Science Center for making calibrated strain data publicly available. Substantial contributions to the data analysis pipeline design, numerical implementation, and interpretation of results were made by Claude (Anthropic, claude-sonnet-4-6), an AI assistant, in the course of an extended research collaboration.

References

[1] B. P. Abbott et al. Observation of gravitational waves from a binary black hole merger. *Physical Review Letters*, 116:061102, 2016.

[2] B. Allen, W. G. Anderson, P. R. Brady, D. A. Brown, and J. D. E. Creighton. FINDCHIRP: An algorithm for detection of gravitational waves from inspiraling compact binaries. *Physical Review D*, 85:122006, 2012.

[3] J. Creswell, S. von Hausegger, A. D. Jackson, H. Liu, and P. Naselsky. On the time lags of the LIGO signals. *Journal of Cosmology and Astroparticle Physics*, 2017:013, 2017.

[4] H. Liu, J. Creswell, S. von Hausegger, A.D. Jackson, and P. Naselsky. A blind search for a common signal in gravitational wave detectors. *arXiv preprint 1802.00340*, 2018.

[5] A. D. Jackson, H. Liu, and P. Naselsky. Noise residuals for GW150914 using maximum likelihood and numerical relativity templates. *Journal of Cosmology and Astroparticle Physics*, 2019:036, 2019.

[6] LIGO Scientific Collaboration and Virgo Collaboration. Gravitational wave open science center. https://gwosc.org, 2023.

[7] B. P. Abbott et al. GW151226: Observation of gravitational waves from a 22-solar-mass binary black hole coalescence. *Physical Review Letters*, 116:241103, 2016.

[8] B. P. Abbott et al. GW170814: A three-detector observation of gravitational waves from a binary black hole coalescence. *Physical Review Letters*, 119:141101, 2017.

[9] P. C. Peters. Gravitational radiation and the motion of two point masses. *Physical Review*, 136:B1224, 1964.

[10] B. P. Abbott et al. GW170817: Observation of gravitational waves from a binary neutron star inspiral. *Physical Review Letters*, 119:161101, 2017.

[11] B. P. Abbott et al. Characterization of transient noise in advanced LIGO relevant to gravitational wave signal GW150914. *Classical and Quantum Gravity*, 33:134001, 2016.

[12] L. K. Nuttall. Characterizing transient noise in the LIGO detectors. *Philosophical Transactions of the Royal Society A*, 376:20170286, 2018.

[13] F. Acernese et al. Increasing the astrophysical reach of the advanced Virgo detector via the application of squeezed vacuum states of light. *Physical Review Letters*, 123:231108, 2019.

[14] B. P. Abbott et al. Multi-messenger observations of a binary neutron star merger. *The Astrophysical Journal Letters*, 848:L12, 2017.